

Research Article

Automatic Seizure Detection Based on Time-Frequency Analysis and Artificial Neural Networks

A. T. Tzallas,^{1,2} M. G. Tsipouras,² and D. I. Fotiadis^{2,3}

¹Department of Medical Physics, Medical School, University of Ioannina, GR 451 10 Ioannina, Greece

²Unit of Medical Technology and Intelligent Information Systems, Department of Computer Science, University of Ioannina, GR 451 10 Ioannina, Greece

³Biomedical Research Institute, Foundation for Research and Technology-Hellas (BRI-FORTH), University of Ioannina, GR 451 10 Ioannina, Greece

Correspondence should be addressed to D. I. Fotiadis, fotiadis@cs.uoi.gr

Received 31 December 2006; Revised 16 July 2007; Accepted 7 October 2007

Recommended by Saied Sanei

The recording of seizures is of primary interest in the evaluation of epileptic patients. Seizure is the phenomenon of rhythmicity discharge from either a local area or the whole brain and the individual behavior usually lasts from seconds to minutes. Since seizures, in general, occur infrequently and unpredictably, automatic detection of seizures during long-term electroencephalograph (EEG) recordings is highly recommended. As EEG signals are nonstationary, the conventional methods of frequency analysis are not successful for diagnostic purposes. This paper presents a method of analysis of EEG signals, which is based on time-frequency analysis. Initially, selected segments of the EEG signals are analyzed using time-frequency methods and several features are extracted for each segment, representing the energy distribution in the time-frequency plane. Then, those features are used as an input in an artificial neural network (ANN), which provides the final classification of the EEG segments concerning the existence of seizures or not. We used a publicly available dataset in order to evaluate our method and the evaluation results are very promising indicating overall accuracy from 97.72% to 100%.

Copyright © 2007 A. T. Tzallas et al. This is an open access article distributed under the Creative Commons Attribution License, which permits unrestricted use, distribution, and reproduction in any medium, provided the original work is properly cited.

1. INTRODUCTION

Epilepsy is one of the most common neurological disorders with a prevalence of 0.6–0.8% of the world's population. Two-thirds of the patients achieve sufficient seizure control from anticonvulsive medication, and another 8–10% could benefit from resective surgery. For the remaining 25% of patients, no sufficient treatment is currently available [1]. The epilepsy is characterized by a sudden and recurrent malfunction of the brain, which is termed “seizure.” Epileptic seizures reflect the clinical signs of an excessive and hyper-synchronous activity of neurons in the brain. Depending on the extent of the involvement of other brain areas during the course of the seizure, epilepsies can be divided into two main classes. Generalized seizures involve almost the entire brain, while focal (or partial) seizures originate from a circumscribed region of the brain (epileptic focus) and remain restricted to this region. Epileptic seizures may be accompa-

nied by impairment or loss of consciousness: psychic, autonomic or sensory symptoms, or motor phenomena [2, 3].

Traditionally, suspected seizures are evaluated using a routine electroencephalogram (EEG), which is typically a 20-minute recording of the patient's brain waves. Because a routine EEG is of short duration, it is unlikely that actual events are recorded. Routine EEGs may record interictal hallmarks of epilepsy, including spikes, sharp waves, or spike-and-wave complexes. However, diagnostic difficulties arise when a person has a suspected seizure, or a neurological event of unclear etiology, not obvious in the routine EEG. The current gold standard is the continuous EEG recording along with video monitoring of the patient, which usually requires inpatient admission. This is a costly endeavour, which is not always available. The patient is away from his environment and routine, which may be associated with factors that provoke the patient's events [4]. The introduction of portable recording systems (ambulatory EEG), however, has allowed

out-patient EEG recording to become more common. This has the advantage that patients are monitored in their normal environment without the reduction in seizure frequency usually occurring during in-patient sessions [4, 5].

Clinical neurophysiologists can then periodically review the EEG recordings and analyze the seizures that may have occurred during the monitoring session. However, reviewing a continuous EEG recording lasting several days can be a time-consuming process. In practice, the patient can indicate that a seizure occurs through the use of an alarm button, so that only the recording sections around the use of the button need to be analyzed. Unfortunately, in many cases, patients are not aware of the occurrence of their own seizures. An automated seizure detection system can thus be of great interest in identifying EEG sections that need to be reviewed. The main difficulty with it lies in the wide variety of EEG patterns that can characterize a seizure, such as “low-amplitude desynchronization, polyspike activity, rhythmic waves for a wide variety of frequencies and amplitudes, and spikes and waves” [6]. In extracranial recordings, EMG, movement, and eye blink artefacts often obscure seizures. Thus, from the pattern recognition point of view, the problem is extremely complex.

Research in automated seizure detection began in the 1970s and various algorithms addressing this problem [5–7] have been presented. Methods for automatic detection of seizures may rely on the identification of various patterns such as an increase in amplitude [8], sustained rhythmic activity [9, 10], or EEG flattening [11]. Several algorithms have been developed based on spectral [12–18] or wavelet features [19–23], amplitude relative to background activity [12, 24] and spatial context [24–27]. Chaotic features [28–31] such as correlation dimension [32, 33], Lyapunov exponents [34], and entropy [35] have also been proposed to characterize the EEG signal. These features can then be used to classify the EEG signal using statistical methods [28–30], nearest neighbour classifiers [36], decision trees [16], ANNs [21, 34], support vector machines (SVMs) [18, 37], or adaptive neuro-fuzzy inference systems [23, 35] in order to identify the occurrence of seizures. It is crucial for seizure detection systems to result in high sensitivity, even if this results in a large number of false detections. Such systems can then be used to reduce considerably the amount of data that need to be reviewed; neurophysiologists can then easily discard false detections.

In addition, to seizure detection systems, warning systems have also become increasingly valuable since detection of seizures at an early stage can warn the patient that a seizure is occurring. Also, they alert medical staff, and allow them to perform behavioral testing to further assess which specific functions may be impaired as a result of a seizure and help them in localizing the source of the seizure activity. Techniques used to forecast seizures include time-domain analysis [38], frequency-based methods [39], nonlinear dynamics and chaos [31, 40], methods of delays [41], and intelligent systems [42]. Advances in seizure prediction promise to give rise to implantable devices able to warn of impending seizures and to trigger therapy to prevent clinical epileptic attacks [2]. Treatments such as electrical stimulation of focal

drug infusion could be given on demand and might eliminate side effects in some patients taking antiepileptic drugs.

Consequently, epileptic seizures give rise to changes in certain frequencies bands. Recent works have focused on the analysis of the δ (0.4–4 Hz), θ (4–8 Hz), α (8–12 Hz), β (12–30 Hz) rhythms, and their relation to epilepsy. An epileptic signal is nonstationary, having time-varying frequency components. Time-frequency (TF) representations combine both time and frequency information into a single representation and have proven to be powerful tools for the analysis of nonstationary signals [43], and have been used for neonatal seizure detection [44, 45].

In this work, we use TF analysis in order to extract several features from EEG segments, and subsequently use these features to classify the segments concerning epileptic seizures. The method is divided into three stages. Initially, TF analysis is performed for each EEG segment and its spectrum is acquired. Then, several features are extracted from it, measuring the fractional energy on specific TF windows. For this purpose, several partitions on the time axis and the frequency axis are tested. Finally, these features are used as inputs in an ANN, which provides the final classification according to the specified number of categories. A dataset of 500 EEG segments is used, while the method is evaluated for four different classification problems, each of them addressing a different interpretation of the medical problem and thus different selection of EEGs from the whole EEG segment dataset is required for each classification problem. TF analysis and feature extraction, reflecting the energy distribution over the TF plane, have been employed only for neonatal epileptic seizure detection and have not been previously applied in general epileptic seizure detection. In addition, no work addresses all four classification problems, which are directly related to the diagnosis provided by an expert. The obtained results indicate high accuracy compared to other existing approaches.

The rest of the paper is structured as follows. In Section 2, the dataset used in our work along with the employed methodology is described in detail. Then, the evaluation procedure and the obtained results are presented (Section 3), followed by an extensive discussion regarding them (Section 4). Finally, some concluding remarks are included in Section 5.

2. MATERIALS AND METHODS

The flowchart of the proposed method is shown in Figure 1. Below the dataset and its partitions used are briefly discussed and the three stages (time-frequency analysis, feature extraction, and classification) of the method are explained in detail.

2.1. Dataset

An EEG dataset, which is available online [46] and includes recordings for both healthy and epileptic subjects, is used. The dataset includes five subsets (denoted as Z, O, N, F, and S) each containing 100 single-channel EEG segments, each one having 23.6-second duration. The subsets Z and O have been acquired using surface EEG recordings of five healthy volunteers with eyes open and closed, respectively. Signals in

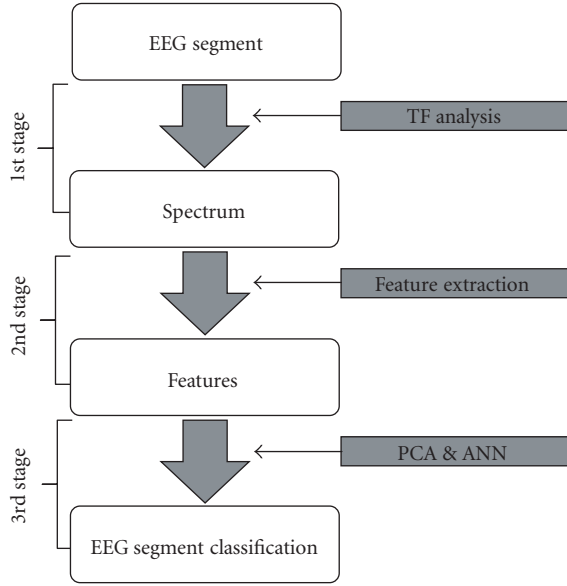


FIGURE 1: The flowchart of the proposed method.

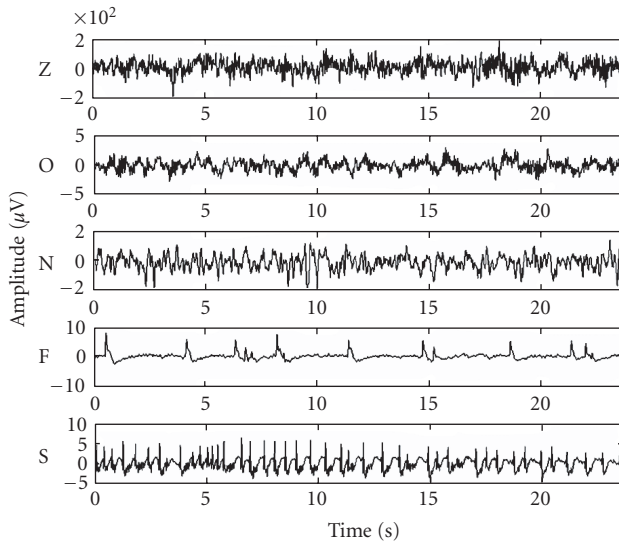


FIGURE 2: Exemplary EEG segments from each of the five subsets (Z, O, N, F, and S). From top to bottom: subset Z to subset S. The amplitudes of surface EEG recordings are typically in the order of some μV . For intracranial EEG recordings, the amplitudes range around $100 \mu\text{V}$. For seizure activity, these voltages can exceed $1000 \mu\text{V}$.

two sets have been measured in seizure-free intervals from five patients in the epileptogenic zone (set F) and from the hippocampal formation of the opposite hemisphere of the brain (set N). Finally, subset S contains seizure activity, selected from all recording sites exhibiting ictal activity. Subsets Z and O have been recorded extracranially, using standard electrode positioning (according to the international 10–20 system [47]), whereas subsets N, F, and S have been recorded intracranially. More specifically, depth electrodes are implanted symmetrically into the hippocampal forma-

tion. EEG segments of subsets N and F were taken from all contacts of the relevant depth electrode [46]. In addition, strip electrodes are implanted onto the lateral and basal regions (middle and bottom) of the neocortex. EEG segments of the subsets S were taken from contacts of all electrodes (depth and strip). All EEG signals were recorded with the same 128-channel amplifier system, using an average common reference. The data were digitized at 173.61 samples per second using 12 bit resolution and they have the spectral bandwidth of the acquisition system, which varies from 0.5 Hz to 85 Hz. Typical EEG segments (one from each category of the dataset) are shown in Figure 2.

In our analysis, we use the above-described dataset to create four different classification problems and then we tested our method with all of them.

- (1) In the first, all the EEG segments from the dataset were used and they were classified into three different classes: Z and O types of EEG segments were combined to a single class, N and F types were also combined to a single class, and type S was the third class. This set is the one closest to real medical applications including three categories; normal (i.e., types Z and O), seizure-free (i.e., types N and F) and seizure (i.e., type S).
- (2) In the second, again all the EEG segments from the dataset were used and they were classified into two different classes: Z, O, N, and F types are included in the first class and type S in the second class. This is also close to real medical applications, being slightly simpler than the previous, classifying the EEG segments into nonseizures and seizures.
- (3) The third has similar classes with the first, that is, normal, seizure-free and seizure, but not all the EEG segments from the dataset were employed. The normal class includes only the Z-type EEG segments, the seizure-free class the F-type EEG segments, and the seizure class the S-type.
- (4) The fourth has similar classes with the second, that is, normal and seizure, but again not all the EEG segments from the dataset were employed. The normal class includes only the Z-type EEG segments while the seizure class includes the S-type.

The above classification problems are shown in detail in Table 1.

2.2. Time-frequency analysis

In the proposed method, the smoothed pseudo-Wigner-Ville distribution (SPWVD) [48, 49] is applied to each EEG segment, defined as

$$\begin{aligned} \text{SPWVD}_x(t, \omega) &= \int_{-\infty}^{+\infty} h(\tau) \left(\int_{-\infty}^{+\infty} g(s-t) x\left(s + \frac{\tau}{2}\right) x^*\left(s - \frac{\tau}{2}\right) ds \right) e^{-j2\pi\omega\tau} d\tau, \end{aligned} \quad (1)$$

where $x(\cdot)$ is the signal, t is the time, ω is the frequency, and $g(\cdot)$ and $h(\cdot)$ are time and frequency smoothing window functions, respectively. SPWVD can substantially suppress

TABLE 1: The classes and the corresponding number of EEG segments of the four classification problems.

Classification problem	Classes	Number of EEG segments
1	Normal (Z, O)	200
	Seizure-free (N, F)	200
	Seizure (S)	100
	Total	500
2	Nonseizure (Z, O, N, F)	400
	Seizure (S)	100
	Total	500
3	Normal (Z)	100
	Seizure-free (N)	100
	Seizure (S)	100
	Total	300
4	Normal (Z)	100
	Seizure (S)	100
	Total	200

TABLE 2: The frequency ranges (Hz) of four frequency subbands (4, 5, 7, and 13).

	Frequency subbands			
	4	5	7	13
	0–4	0–2.5	0–2	0–2
	4–8	2.5–5.5	2–4	2–4
	8–12	5.5–10.5	4–6.5	4–6
	12–40	10.5–21.5	6.5–9	6–8
	—	21.5–43.5	9–12	8–10
	—	—	12–25	10–12
Frequency ranges (Hz)	—	—	25–40	12–16
	—	—	—	16–20
	—	—	—	20–24
	—	—	—	24–28
	—	—	—	28–32
	—	—	—	32–36
	—	—	—	36–40

the cross terms, which is a major limitation of the time-frequency analysis. The time smoothing window was selected to be a Hamming 64-point length window, which was the same for all tests performed for evaluation. The length of the frequency smoothing window is not always the same; we have selected several different frequency resolutions (64, 128, 256, and 512 points length window), and we tested the method for all of them. Time-frequency (TF) analysis is used to calculate the spectrum of the signal. Figure 3 shows the spectrum of five EEG segments, one of each of the original dataset categories (Z, O, N, F, and S), using a 512-point length window.

2.3. Feature extraction

The spectrum of the signals, computed using TF analysis, is used to extract several features. To do that, a grid is used,

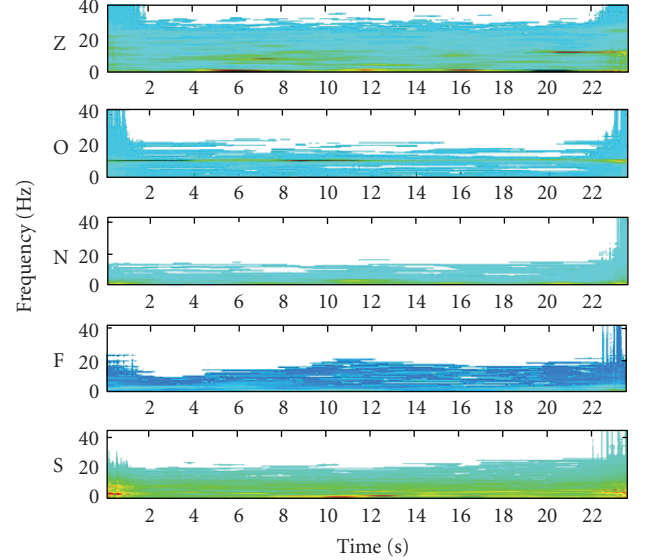


FIGURE 3: The obtained spectrum for five EEG segments, one for each of the original dataset categories (Z, O, N, F, and S).

based on a time and a frequency partition. In the time domain, two different partitions were used, having three and five equal-sized windows, respectively, while in the frequency domain, four different partitions were used, which divide the frequency domain in 4, 5, 7, and 13 subbands. These subbands, which are not always equal, are shown in Table 2 and they are created using medical knowledge about the EEG and the features that are expected to be found in certain frequency bands for the specific types of EEG segments included in the original dataset. All the combinations between these time and frequency partitions are used, in order to extract several sets of features. The result of the application of TF analysis in an EEG segment for different combinations of time windows and frequency subbands is shown in Figure 4.

Each feature, $f(i, j)$, is calculated as

$$f(i, j) = \int_{t_i} \int_{\omega_j} \text{SPWVD}_x(t, \omega) d\omega dt, \quad (2)$$

where t_i is the i th time window and ω_j is the j th frequency band. Each feature represents the fractional energy of the signal in a specific frequency band and time window; thus the total feature set depicts the distribution of the signal's energy over the TF plane. Therefore, it is expected that each feature set carries sufficient information related to the nonstationary properties of the signal and thus, it can be useful for the classification process. The feature set initially is represented as an $N \times M$ matrix, where N is the number of time windows and M is the number of frequency subbands, and then it is reshaped into an $N \cdot M$ size vector. The length of the feature vector is not the same in all cases and it depends only on the time and frequency partitions. In all cases, an additional feature is used, which is the total energy of the signal. Thus, in each case the total number of features is $N \cdot M + 1$.

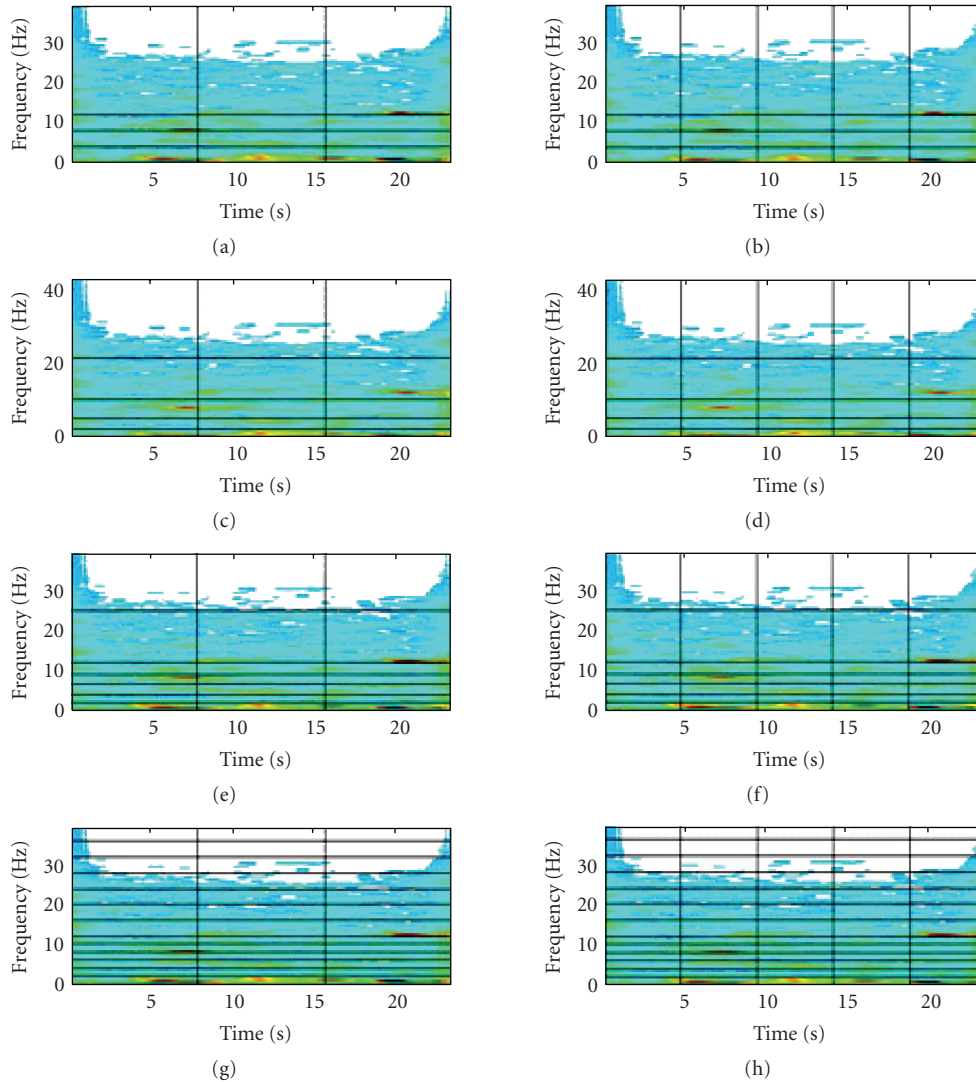


FIGURE 4: The spectrums obtained for various combinations of time and frequency partitions: (a) 3 time windows and 4 frequency subbands, (b) 5 time windows and 4 frequency subbands, (c) 3 time windows and 5 frequency subbands, (d) 5 time windows and 5 frequency subbands, (e) 3 time windows and 7 frequency subbands, (f) 5 time windows and 7 frequency subbands, (g) 3 time windows and 13 frequency subbands, and (h) 5 time windows and 13 frequency subbands.

2.4. Classification

The calculated features are fed into a feed-forward artificial neural network (ANN). To reduce the dimensionality of the input patterns, principal component analysis (PCA) is employed with the threshold set to 1%. The architecture of the neural network is different in each classification problem: N inputs (N is the number of features resulted from the PCA), one hidden layer with $4 \cdot N$ neurons, and M outputs (M is the number of the classes), each of them being a real number in the interval $[0, 1]$. The units in the hidden layer are sigmoid units with hyperbolic tangent as activation function, while the outputs are linear. Half of the patterns of the dataset were randomly selected to be used for training, while the rest were used for testing. The network is trained using a standard backpropagation algorithm [50]. Ten different training-test

sets were created for each classification problem and thus ten different neural networks were optimized. The final result is obtained as the average of their results.

3. RESULTS

The four classification problems, described above, are used to evaluate the proposed method. For each of them, all combinations between frequency resolutions (64, 128, 256, or 512), time windows (3 or 5), and frequency bands (4, 5, 7, or 13) were tested; totally 32 different combinations for each classification problem. For each problem, half of the EEG segments, randomly selected, were used for the training of the neural network, while the other half for testing.

The size of the confusion matrix depends on the classification problem: 3×3 for problems (1) and (3), 2×2 for

TABLE 3: Results for the first classification problem, in terms of sensitivity (Sens), specificity (Spec), and selectivity (Sel) in % values. Those are given for all TF resolutions (64, 128, 256, and 512), time windows (3 and 5), and frequency subbands (4, 5, 7, and 13).

Frequency subbands			4			5			7			13		
Classes			ZO	NF	S	ZO	NF	S	ZO	NF	S	ZO	NF	S
Frequency resolution 64	Time windows 3	Sens	98.90	94.20	97.00	97.90	96.80	95.60	95.80	93.20	93.80	96.10	97.80	90.80
		Spec	98.00	98.53	98.40	97.53	97.80	99.75	95.67	95.80	99.35	98.27	95.53	99.30
		Sel	97.06	97.72	93.81	96.36	96.70	98.96	93.65	93.67	97.30	97.37	93.59	97.01
	Time windows 5	Sens	95.40	91.90	90.80	95.70	95.50	88.80	96.20	92.90	92.20	93.30	93.30	88.60
		Spec	95.53	95.07	98.40	96.20	94.40	99.85	96.27	96.27	98.20	95.33	93.87	98.55
		Sel	93.44	92.55	93.42	94.38	91.92	99.33	94.50	94.31	92.76	93.02	91.02	93.86
Frequency resolution 128	Time windows 3	Sens	99.20	95.50	97.40	97.90	95.20	91.20	99.60	96.90	94.60	96.80	93.20	87.40
		Spec	97.60	98.87	99.35	96.80	96.80	99.15	98.00	98.13	99.80	95.47	95.47	98.65
		Sel	96.50	98.25	97.40	95.33	95.20	96.41	97.08	97.19	99.16	93.44	93.20	94.18
	Time windows 5	Sens	95.90	92.70	97.40	96.80	93.10	92.00	96.30	93.60	89.80	96.20	91.60	93.00
		Spec	96.73	96.47	98.75	95.67	96.40	98.90	95.33	96.07	98.85	94.93	97.60	97.75
		Sel	95.14	94.59	95.12	93.71	94.52	95.44	93.22	94.07	95.13	92.68	96.22	91.18
Frequency resolution 256	Time windows 3	Sens	96.60	95.70	98.00	98.20	90.80	87.20	98.00	96.00	96.20	96.50	98.00	93.00
		Spec	98.27	97.20	99.05	93.53	95.87	99.25	97.20	97.93	99.70	97.60	97.67	99.05
		Sel	97.38	95.80	96.27	91.01	93.61	96.67	95.89	96.87	98.77	96.40	96.55	96.07
	Time windows 5	Sens	95.20	93.50	93.80	94.90	92.40	89.80	94.00	91.90	92.80	96.80	92.00	85.00
		Spec	96.80	95.40	98.65	95.27	94.13	99.05	95.53	94.73	98.45	92.47	97.33	98.30
		Sel	95.20	93.13	94.56	93.04	91.30	95.94	93.35	92.08	93.74	89.55	95.83	92.59
Frequency resolution 512	Time windows 3	Sens	97.50	95.00	93.80	98.50	97.30	91.60	97.30	95.70	96.40	98.80	99.00	93.00
		Spec	98.20	96.67	98.55	97.33	98.13	99.20	98.53	97.20	98.80	98.20	98.20	99.85
		Sel	97.31	95.00	94.18	96.10	97.20	96.62	97.79	95.80	95.26	97.34	97.35	99.36
	Time windows 5	Sens	95.70	90.20	95.80	95.60	92.70	90.00	92.30	90.40	90.00	96.00	95.70	83.20
		Spec	95.47	96.27	98.10	95.27	95.93	98.25	93.60	93.27	98.70	95.67	94.13	99.30
		Sel	93.37	94.15	92.65	93.09	93.83	92.78	90.58	89.95	94.54	93.66	91.58	96.74

problems (2) and (4). Results for each class i are derived in terms of sensitivity (Sens), specificity (Spec), and selectivity (Sel):

$$\text{Sens}_i = \frac{\text{Number of patterns of class } i \text{ classified in class } i}{\text{Total number of patterns in class } i}, \quad (3)$$

$$\text{Spec}_i = \frac{\text{Number of patterns not in class } i \text{ classified not in class } i}{\text{Total number of patterns not in class } i}, \quad (4)$$

$$\text{Sel}_i = \frac{\text{Number of patterns of class } i \text{ classified in class } i}{\text{Total number of patterns classified in class } i}. \quad (5)$$

The results for the classification problems (1)–(4) are shown in Tables 3–6, respectively.

The accuracy (Acc), defined as

$$\text{Acc} = \text{Trace}(\text{cm}), \quad (6)$$

where cm is the confusion matrix, defined as

$$\text{cm}_{i,j} = \text{number of patterns belonging to class } i \text{ and classified to class } j, \quad (7)$$

is calculated for each confusion matrix. The computed accuracies, along with the standard deviations are presented in Table 7. Additionally, the initial number of features and the reduced number of features after the PCA application are presented. For each classification problem, overall results have been derived, that is, the maximum and minimum accuracies (for all combinations between frequency resolutions, time windows, and frequency subbands) as well as the average accuracy and the standard deviation. For the first classification problem, the best obtained accuracy is 97.72%, achieved for 512 frequency resolution, 3 time windows, and 13 frequency subbands. For the second classification problem, the best obtained accuracy is 97.73%, achieved for 512 frequency resolution, 3 time windows, and 5 frequency subbands. For the third classification problem, the best obtained accuracy is 99.28%, achieved for 128 frequency resolution, 3 time windows, and 4 frequency subbands. Finally, for the fourth classification problem, the best obtained accuracy is 100%, achieved in most of the cases; in 28 out of 32 different

TABLE 4: Results for the second classification problem, in terms of sensitivity (Sens), specificity (Spec), and selectivity (Sel) in % values. Those are given for all TF resolutions (64, 128, 256, and 512), time windows (3 and 5), and frequency subbands (4, 5, 7, and 13).

Frequency subbands			4		5		7		13			
Classes			ZONF	S	ZONF	S	ZONF	S	ZONF	S		
Frequency resolution	64	Time windows	3	Sens	98.40	97.60	98.55	95.60	99.30	96.00	99.10	92.40
				Spec	97.60	98.40	95.60	98.55	96.00	99.30	92.40	99.10
			Sel	99.39	93.85	98.90	94.28	99.00	97.17	98.12	96.25	
		5	Sens	97.70	97.00	99.35	93.20	98.70	91.80	98.65	91.80	
			Spec	97.00	97.70	93.20	99.35	91.80	98.70	91.80	98.65	
			Sel	99.24	91.34	98.32	97.29	97.97	94.64	97.96	94.44	
Frequency resolution	128	Time windows	3	Sens	99.50	98.40	99.25	92.60	99.55	96.80	98.05	92.40
				Spec	98.40	99.50	92.60	99.25	96.80	99.55	92.40	98.05
			Sel	99.60	98.01	98.17	96.86	99.20	98.17	98.10	92.22	
		5	Sens	99.50	97.80	99.05	92.80	98.95	93.20	98.10	94.80	
			Spec	97.80	99.50	92.80	99.05	93.20	98.95	94.80	98.10	
			Sel	99.45	98.00	98.22	96.07	98.31	95.69	98.69	92.58	
Frequency resolution	256	Time windows	3	Sens	99.25	99.00	98.90	86.40	99.45	96.60	99.40	93.60
				Spec	99.00	99.25	86.40	98.90	96.60	99.45	93.60	99.40
			Sel	99.75	97.06	96.68	95.15	99.15	97.77	98.42	97.50	
		5	Sens	98.55	96.20	99.00	94.40	98.70	94.20	97.15	92.60	
			Spec	96.20	98.55	94.40	99.00	94.20	98.70	92.60	97.15	
			Sel	99.05	94.31	98.61	95.93	98.55	94.77	98.13	89.04	
Frequency resolution	512	Time windows	3	Sens	98.90	96.20	99.05	94.20	98.85	95.60	99.70	94.20
				Spec	96.20	98.90	94.20	99.05	95.60	98.85	94.20	99.70
			Sel	99.05	95.63	98.56	96.12	98.90	95.41	98.57	98.74	
		5	Sens	98.35	95.00	98.65	92.60	98.75	93.40	98.85	89.20	
			Spec	95.00	98.35	92.60	98.65	93.40	98.75	89.20	98.85	
			Sel	98.74	93.50	98.16	94.49	98.36	94.92	97.34	95.10	

evaluations of the fourth classification problem we obtained accuracy 100%.

For the first two classification problems, the obtained accuracies of the different evaluations varied significantly; almost 6.5% (max-min) for both of them, with average 95% and standard deviation 1.7%. For the third classification problem, the max-min difference is 3% and the average 97.94%, with 0.75% standard deviation. Finally, for the fourth classification problem, the max-min difference is 1.3% and the average 99.92%, with 0.26% standard deviation.

4. DISCUSSION

We have proposed an automated method for seizure detection in EEG recordings. The method is based on TF analysis of the EEG segments and extraction of several features from the spectrum of the signal. These features are fed into neural networks, which provide the final classification of the EEG segments. The method is evaluated using four different classification problems originated from the type of medical diagnosis, which can be obtained. The effect of different parameters of the method on the classification accuracy is exam-

ined. Those parameters are the frequency resolution of the TF analysis, the length of the time window, and the width of the frequency subbands used in the feature extraction. The different combinations among all the afore-mentioned parameters result in a large number of different experimental settings (32) for each classification problem (4) and 10 different realizations (selections of training/test datasets) for each of them—totally 1280 optimized and evaluated ANNs—and results are presented for all of them. This is considered an extensive validation procedure, which can sufficiently exploit the potentials of the proposed method.

In this method, the SPWVD has been employed for the TF analysis of the EEG signals. Other distributions have been also tried but the better results were obtained for SPWVD.

The frequency resolution, used in the TF analysis, does not greatly affect the accuracy of the proposed method; the average accuracies of all different combinations of time windows and frequency subbands, for the four classification problems, are 96.71%, 97.13%, 96.7%, and 96.87% for 64, 128, 256, and 512 points length windows, respectively. It is obvious that the use of 128 points length window slightly improves the results. On the other hand, the number of the time windows is important for the analysis; in the case of three

TABLE 5: Results for the third classification problem, in terms of sensitivity (Sens), specificity (Spec), and selectivity (Sel) in % values. Those are given for all TF resolutions (64, 128, 256, and 512), time windows (3 and 5), and frequency subbands (4, 5, 7, and 13).

Frequency subbands		4			5			7			13			
Classes		Z	F	S	Z	F	S	Z	F	S	Z	F	S	
Frequency resolution 64	Time windows 3	Sens	99.00	93.80	96.60	97.80	95.20	98.20	97.00	87.80	97.80	97.40	98.00	93.20
		Spec	98.90	97.80	98.00	98.60	98.50	98.50	94.60	98.30	98.40	99.30	94.60	98.90
		Sel	97.83	95.52	96.02	97.22	96.95	97.04	89.98	96.27	96.83	98.54	90.07	97.69
	Time windows 5	Sens	94.60	84.20	96.40	96.40	92.40	92.80	95.20	92.80	94.80	90.20	90.60	93.60
		Spec	94.50	96.20	96.90	95.80	95.30	99.70	97.40	95.50	98.50	96.40	92.80	98.00
		Sel	89.58	91.72	93.96	91.98	90.77	99.36	94.82	91.16	96.93	92.61	86.29	95.90
Frequency resolution 128	Time windows 3	Sens	99.20	90.60	97.40	99.40	93.40	92.80	99.40	98.60	93.00	97.40	95.80	93.40
		Spec	96.50	98.50	98.60	97.00	97.50	98.30	98.60	97.50	99.40	98.50	96.40	98.40
		Sel	93.41	96.79	97.21	94.31	94.92	96.47	97.26	95.17	98.73	97.01	93.01	96.69
	Time windows 5	Sens	95.40	91.60	95.60	98.20	96.20	92.20	95.00	95.40	95.20	96.40	90.60	94.00
		Spec	97.30	95.60	98.40	97.80	96.00	99.50	98.30	96.00	98.50	95.40	97.80	97.30
		Sel	94.64	91.24	96.76	95.71	92.32	98.93	96.54	92.26	96.95	91.29	95.37	94.57
Frequency resolution 256	Time windows 3	Sens	92.00	92.80	98.80	99.20	96.20	92.60	96.40	96.00	94.00	98.20	97.80	95.20
		Spec	97.90	95.40	98.50	97.90	96.50	99.60	97.80	96.60	98.80	98.40	97.80	99.40
		Sel	95.63	90.98	97.05	95.94	93.22	99.14	95.63	93.39	97.51	96.84	95.69	98.76
	Time windows 5	Sens	95.60	91.40	95.40	90.20	92.80	94.40	94.20	91.00	92.40	98.40	91.80	97.00
		Spec	97.40	95.70	98.10	97.10	93.00	98.60	95.70	94.50	98.60	96.60	98.20	98.80
		Sel	94.84	91.40	96.17	93.96	86.89	97.12	91.63	89.22	97.06	93.54	96.23	97.59
Frequency resolution 512	Time windows 3	Sens	99.80	95.20	96.20	99.60	97.40	96.20	94.20	94.20	94.60	99.40	96.40	93.80
		Spec	98.20	98.30	99.10	98.40	98.60	99.60	98.00	95.20	98.30	98.30	97.30	99.20
		Sel	96.52	96.55	98.16	96.89	97.21	99.18	95.93	90.75	96.53	96.69	94.70	98.32
	Time windows 5	Sens	97.60	85.80	95.40	98.00	91.20	94.00	91.40	92.60	96.40	96.20	94.00	89.40
		Spec	94.70	96.60	98.10	97.50	96.50	97.60	97.90	94.50	97.80	96.50	94.20	99.10
		Sel	90.20	92.66	96.17	95.15	92.87	95.14	95.61	89.38	95.63	93.22	89.02	98.03

time windows, the average accuracy of all different combinations between the frequency resolutions and frequency subbands, for all four classification problems, is 97.52%, while the accuracy in the case of five time windows is 96.2%. This means that analyzing EEG segments of approximately 8-second length reveals more information for the epileptic seizures than having 5-second windows. Other statistical measurements lead to the same conclusion; in the case of three time windows, the minimum accuracy of all cases is 93.04% and the standard deviation 1.8%, while the accuracy for five time windows is 91.08% and the standard deviation 2.9%, respectively. Finally, concerning the number of frequency subbands, again the reported average accuracies for all combinations among the frequency resolutions and the time windows, for all classification problems, are 97.07%, 96.87%, 96.84%, and 96.62% for 4, 5, 7, and 13 frequency subbands, respectively. This gives indications that the separation in δ , θ , α , and β rhythms is the one that mostly detects the TF components that characterize the signal regarding epileptic seizures, compared to 5 and 7, which have been used in other methods [20, 22], and 13, which is defined in this work to examine if a frequency resolution with a large number of frequency subbands improves the classification

accuracy. The results indicate that all selections for frequency subbands result in similar high-average accuracies—the difference between the best and worst average accuracy is 0.45%. This can be justified since they are generated either based on expert knowledge or have been previously proposed in the literature. Concerning the frequency subbands, the higher their number, is the lower (slightly) the average accuracy obtained.

To our knowledge, TF analysis and feature extraction, which reflect the energy over the TF plane, have been only applied in the analysis of neonatal EEG signals (and mainly for neonatal epileptic seizure detection) and not EEG signals in general. Moreover, the quality of the proposed method can be proved from the obtained results. The accuracy achieved by our method for the epileptic seizure detection is more than satisfactory and also its automated nature makes it suitable to be used in real clinical conditions. Besides the feasibility of a real-time implementation of the proposed method, the diagnosis can be made more accurate by increasing the number of parameters. A system that may be developed as a result of this study may provide feedback to the experts for classification of the EEG signals quickly and accurately by examining the EEG signal.

TABLE 6: Results for the fourth classification problem, in terms of sensitivity (Sens), specificity (Spec), and selectivity (Sel) in % values. Those are given for all TF resolutions (64, 128, 256, and 512), time windows (3 and 5), and frequency subbands (4, 5, 7, and 13).

			Frequency subbands		4		5		7		13		
			Classes		Z	S	Z	S	Z	S	Z	S	
Frequency resolution	64	Time windows	3	Sens	100	100	100	100	100	100	100	100	
				Spec	100	100	100	100	100	100	100	100	
				Sel	100	100	100	100	100	100	100	100	
			5	Sens	100	100	100	100	100	100	100	100	100
				Spec	100	100	100	100	100	100	100	100	100
				Sel	100	100	100	100	100	100	100	100	100
Frequency resolution	128	Time windows	3	Sens	100	100	100	100	100	100	100	99.80	
				Spec	100	100	100	100	100	100	100	99.80	100
				Sel	100	100	100	100	100	100	100	99.80	100
			5	Sens	100	100	100	100	100	100	100	100	100
				Spec	100	100	100	100	100	100	100	100	100
				Sel	100	100	100	100	100	100	100	100	100
Frequency resolution	256	Time windows	3	Sens	100	100	99.80	97.60	100	100	100	98.80	
				Spec	100	100	97.60	99.80	100	100	98.80	100	
				Sel	100	100	97.65	99.80	100	100	98.81	100	
			5	Sens	100	100	100	100	100	100	100	100	100
				Spec	100	100	100	100	100	100	100	100	100
				Sel	100	100	100	100	100	100	100	100	100
Frequency resolution	512	Time windows	3	Sens	100	100	100	100	100	100	100	99.00	
				Spec	100	100	100	100	100	100	99.01	100	
				Sel	100	100	100	100	100	100	99.01	100	
			5	Sens	100	100	100	100	100	100	100	100	100
				Spec	100	100	100	100	100	100	100	100	100
				Sel	100	100	100	100	100	100	100	100	100

Table 8 presents a comparison between our method and other methods proposed in the literature. Only methods evaluated in the same dataset are included so that a comparison between the results is feasible. For the two classes' problem, using only the Z and S types of EEG segments, the results obtained from the evaluation of our method are the best presented for this dataset. The difference between our result and all other results proposed in the literature varies from 0.4% to 10%. The second two classes' problem that we used to evaluate our method also presents high-accuracy results (97.73%). It is worth to mention here that a method that discriminates EEGs into nonseizure and seizure is much closer to the expert needs.

Regarding the three classes' problem, the results obtained from our method are the best presented for this dataset, either using only the Z, F, and S types or all the available dataset. In the case of using the third problem to evaluate our method (i.e., only the Z, F, and S types), the difference between our results and all others' results varies from 2.5% to 13.4%. In the case of using the first classification problem to evaluate our method (i.e., the Z and O, F and N, S types), the difference between our results and all others' results ranges from 1% to 12%. The second case has also the advantage of

being a more realistic classification, dividing the dataset to normal, seizure-free, and seizure EEGs, and thus being closer to clinical conditions.

Still, however, there are several other aspects either technical or medical which must be addressed. From the technical point of view, although we have examined the effect of various parameters (frequency resolution, number of time windows, and frequency bands), some other, like time-frequency distributions (e.g., reduced interference distributions), have not been explored. Furthermore, we mainly focused on the effects of the parameters related to frequency analysis, either for the calculation of the spectrum of the signal or for the frequency resolution for feature extraction. More detailed examination of the time resolution for feature extraction may also reveal important information regarding the seizure detection; this feature will be addressed in feature communications. From the medical point of view, the most important feature is that currently the method is used to characterize predetermined (with respect to their length) EEG segments. An important aspect is also the modification of the proposed method in order to be able to automatically detect highly suspicious segments (regardless of their length) into long time EEG recordings and classify them.

TABLE 7: Accuracy (%), standard deviation (in the parenthesis), and initial number of features/reduced number of features after PCA application, for all classification problems (1, 2, 3, and 4) reported, for all TF resolutions (64, 128, 256, and 512), time windows (3 and 5), and frequency subbands (4, 5, 7, and 13).

Frequency resolution	Time windows	Frequency subbands	Classification problem				
			1	2	3	4	
64	3	4	96.64 (0.34) 13/3	96.47(0.45) 13/3	98.24 (0.33) 13/3	100 (0) 13/3	
		5	97 (0.76) 16/3	97.07(0.78) 16/3	97.96 (0.61) 16/3	100 (0) 16/3	
		7	94.36 (0.58) 22/5	94.2 (0.89) 22/5	98.64 (0.34) 22/5	100 (0) 22/5	
		13	95.72 (0.71) 40/4	95.2 (1.25) 40/4	97.76 (0.33) 40/4	100 (0) 40/4	
	5	4	93.08 (0.96) 21/4	91.73 (0.84) 21/4	97.56 (0.39) 21/4	100 (0) 21/4	
		5	94.24 (0.54) 26/4	93.87 (1.08) 26/4	98.12 (0.6) 26/4	100 (0) 26/4	
		7	94.08 (0.7) 36/4	94.27 (0.95) 36/4	97.32 (0.19) 36/4	100 (0) 36/4	
		13	92.36 (0.81) 66/4	91.47 (0.82) 66/4	97.28 (0.37) 66/4	100 (0) 66/4	
	128	3	4	97.36 (0.34) 13/3	95.73 (0.47) 13/3	99.28 (0.17) 13/3	100 (0) 13/3
			5	95.48 (0.33) 16/3	95.2 (0.61) 16/3	97.92 (0.32) 16/3	100 (0) 16/3
			7	97.52 (0.25) 22/4	97 (0.47) 22/4	99 (0.34) 22/4	100 (0) 22/4
			13	93.48 (0.80) 40/5	95.53 (1.3) 40/5	96.92 (0.42) 40/5	99.9 (0.32) 40/5
5		4	94.92 (0.71) 21/4	94.2 (1.41) 21/4	99.16 (0.35) 21/4	100 (0) 21/4	
		5	94.36 (0.72) 26/4	95.53 (0.71) 26/4	97.8 (0.28) 26/4	100 (0) 26/4	
		7	93.92 (1.1) 36/4	95.2 (0.93) 36/4	97.8 (0.39) 36/4	100 (0) 36/4	
		13	93.72 (0.9) 66/5	93.67 (1.18) 66/5	97.44 (0.47) 66/5	100 (0) 66/5	
256		3	4	96.52 (0.27) 13/3	94.53 (0.42) 13/3	99.2 (0) 13/3	100 (0) 13/3
			5	93.04 (0.78) 16/3	96 (0.7) 16/3	96.4 (0.53) 16/3	98.7 (0.82) 16/3
			7	96.84 (0.35) 22/5	95.47 (0.53) 22/5	98.88 (0.41) 22/5	100 (0) 22/5
			13	96.4 (0.9) 40/6	97.07 (0.84) 40/6	98.24 (0.39) 40/6	99.4 (0.52) 40/6
	5	4	94.24 (0.8) 21/4	94.13 (1.21) 21/4	98.08 (0.53) 21/4	100 (0) 21/4	
		5	92.88 (0.53) 26/5	92.47 (1.18) 26/5	98.08 (0.49) 26/5	100 (0) 26/5	
		7	92.92 (0.6) 36/5	92.53 (0.61) 36/5	97.8 (0.43) 36/5	100 (0) 36/5	
		13	92.52 (0.71) 66/5	95.73 (0.84) 66/5	96.24 (0.63) 66/5	100 (0) 66/5	
	512	3	4	95.76 (0.28) 13/3	97.07 (0.72) 13/3	98.36 (0.4) 13/3	100 (0) 13/3
			5	96.64 (0.34) 16/4	97.73 (1) 16/4	98.08 (0.62) 16/4	100 (0) 16/4
			7	96.48 (0.59) 22/5	94.33 (0.85) 22/5	98.2 (0.28) 22/5	100 (0) 22/5
			13	97.72 (0.38) 40/6	96.53 (0.69) 40/6	98.6 (0.47) 40/6	99.5 (0.53) 40/6
5		4	93.52 (0.67) 21/5	92.93 (0.9) 21/5	97.68 (0.41) 21/5	100 (0) 21/5	
		5	93.32 (0.46) 26/5	94.4 (1.1) 26/5	97.44 (0.43) 26/5	100 (0) 26/5	
		7	91.08 (1.18) 36/5	93.47 (0.88) 36/5	97.68 (0.45) 36/5	100 (0) 36/5	
		13	93.32 (1.16) 66/5	93.2 (1.47) 66/5	96.92 (0.5) 66/5	100 (0) 66/5	
		Total					
		Max	97.72	97.73	99.28	100	
		Min	91.08	91.47	96.24	98.7	
		Average	94.73	94.81	97.94	99.92	
		SD	1.78	1.63	0.75	0.26	

5. CONCLUSIONS

In this paper, we explored the ability of the TF analysis to classify EEG segments which contain epileptic seizures. We have extracted several time-frequency features and we examined the effect of the parameters entering the problem, that is, the frequency resolution of the time-frequency analysis and the number of time windows and frequency subbands used for feature extraction. Promising results have been re-

ported after the evaluation of the proposed method in four different classification problems, derived from a well-known database. However, several types of artefacts have been removed from this database after visual inspection. This is a limitation of the evaluation of our method and thus further evaluation under real clinical conditions is required in order to fully exploit its potential. Another limitation is that in the current study high-frequency components (over 40 Hz) were not measured and thus taken under consideration; the

TABLE 8: A comparison of the results obtained by our method and others' methods (classification accuracy) for two and three categories classification problems.

Classes	Authors (year)	Method	Dataset	Accuracy
2	Nigam et al. [15] (2004)	Nonlinear preprocessing filter, diagnostic artificial neural network (LAMSTAR)	Z, S	97.2
	Srinivasan et al. [14] (2005)	Time & frequency domain features, recurrent neural network (RNN)	Z, S	99.6
	Kannathal et al. [42] (2005)	Entropy measures, adaptive neurofuzzy inference system (ANFIS)	Z, S	92.22
	Kannathal et al. [35] (2005)	Chaotic measures, surrogate data analysis	Z, S	~ 90
	Polat et al. [16] (2006)	Fast Fourier transform (FFT), decision tree (DT)	Z, S	98.72
	Subasi [22] (2007)	Discrete wavelet transform (DWT), mixture of expert model	Z, S	95
	This work (2007)	Time frequency (TF) analysis, artificial neural network (ANN)	Z, S	100
	This work (2007)	Time frequency (TF) analysis, artificial neural network (ANN)	(Z, O, N, F), S	97.73
3	Guler et al. [34] (2005)	Lyapunov exponents, recurrent neural network (RNN)	Z, F, S	96.79
	Sadati et al. [23] (2006)	Discrete wavelet transform (DWT), adaptive neural fuzzy network (ANFN)	Z, F, S	85.9
	This work (2007)	Time frequency (TF) analysis, artificial neural network (ANN)	Z, F, S	99.28
	This work (2007)	Time frequency (TF) analysis, artificial neural network (ANN)	(Z, O), (N, F), S	97.72

employment of high-frequency components, such as gamma activity, and their importance concerning epileptic seizure detection will be addressed in a future communication. Finally, several technical aspects can be further investigated, such as different techniques for feature reduction and alternative classification algorithms.

REFERENCES

- [1] F. Mormann, R. G. Andrzejak, C. E. Elger, and K. Lehnertz, "Seizure prediction: the long and winding road," *Brain*, vol. 130, no. 2, pp. 313–333, 2006.
- [2] B. Litt and J. Echazu, "Prediction of epileptic seizures," *Lancet Neurology*, vol. 1, no. 1, pp. 22–30, 2002.
- [3] K. Lehnertz, F. Mormann, T. Kreuz, et al., "Seizure prediction by nonlinear EEG analysis," *IEEE Engineering in Medicine and Biology Magazine*, vol. 22, no. 1, pp. 57–63, 2003.
- [4] E. Waterhouse, "New horizons in ambulatory electroencephalography," *IEEE Engineering in Medicine and Biology Magazine*, vol. 22, no. 3, pp. 74–80, 2003.
- [5] N. McGrogan, *Neural network detection of epileptic seizures in the electroencephalogram*, Ph.D. thesis, Oxford University, Oxford, UK, February 1999.
- [6] J. Gotman, "Automatic detection of seizures and spikes," *Journal of Clinical Neurophysiology*, vol. 16, no. 2, pp. 130–140, 1999.
- [7] R. O. Sirne, S. I. Isaacson, and C. E. D'Attellis, "A data-reduction process for long-term EEGs: feature extraction through digital processing in a multiresolution framework," *IEEE Engineering in Medicine and Biology Magazine*, vol. 18, no. 1, pp. 56–61, 1999.
- [8] P. F. Prior, R. S. M. Virden, and D. E. Maynard, "An EEG device for monitoring seizure discharges," *Epilepsia*, vol. 14, no. 4, pp. 367–372, 1973.
- [9] J. Gotman, "Automatic recognition of epileptic seizures in the EEG," *Electroencephalography and Clinical Neurophysiology*, vol. 54, no. 5, pp. 530–540, 1982.
- [10] W. R. S. Webber, R. P. Lesser, R. T. Richardson, and K. Wilson, "An approach to seizure detection using an artificial neural network (ANN)," *Electroencephalography and Clinical Neurophysiology*, vol. 98, no. 4, pp. 250–272, 1996.
- [11] G. W. Harding, "An automated seizure monitoring system for patients with indwelling recording electrodes," *Electroencephalography and Clinical Neurophysiology*, vol. 86, no. 6, pp. 428–437, 1993.
- [12] A. M. Murro, D. W. King, J. R. Smith, B. B. Gallagher, H. F. Flanigin, and K. Meador, "Computerized seizure detection of complex partial seizures," *Electroencephalography and Clinical Neurophysiology*, vol. 79, no. 4, pp. 330–333, 1991.
- [13] A. J. Gabor, "Seizure detection using a self-organizing neural network: validation and comparison with other detection strategies," *Electroencephalography and Clinical Neurophysiology*, vol. 107, no. 1, pp. 27–32, 1998.
- [14] V. Srinivasan, C. Eswaran, and A. N. Sriraam, "Artificial neural network based epileptic detection using time-domain and frequency-domain features," *Journal of Medical Systems*, vol. 29, no. 6, pp. 647–660, 2005.
- [15] V. P. Nigam and D. Graupe, "A neural-network-based detection of epilepsy," *Neurological Research*, vol. 26, no. 1, pp. 55–60, 2004.
- [16] K. Polat and S. Güneş, "Classification of epileptiform EEG using a hybrid system based on decision tree classifier and fast

- Fourier transform,” *Applied Mathematics and Computation*, vol. 187, no. 2, pp. 1017–1026, 2007.
- [17] A. Alkan, E. Koklukaya, and A. Subasi, “Automatic seizure detection in EEG using logistic regression and artificial neural network,” *Journal of Neuroscience Methods*, vol. 148, no. 2, pp. 167–176, 2005.
- [18] B. Gonzalez-Vellon, S. Sanei, and J. A. Chambers, “Support vector machines for seizure detection,” in *Proceedings of the 3rd IEEE International Symposium on Signal Processing and Information Technology (ISSPIT '03)*, pp. 126–129, Darmstadt, Germany, December 2003.
- [19] S. Blanco, C. E. D’Attellis, S. I. Isaacson, O. A. Rosso, and R. O. Siraes, “Time-frequency analysis of electroencephalogram series. II. Gabor and wavelet transforms,” *Physical Review E*, vol. 54, no. 6, pp. 6661–6672, 1996.
- [20] H. Adeli, Z. Zhou, and N. Dadmehr, “Analysis of EEG records in an epileptic patient using wavelet transform,” *Journal of Neuroscience Methods*, vol. 123, no. 1, pp. 69–87, 2003.
- [21] A. Subasi, A. Alkan, E. Koklukaya, and M. K. Kiyimik, “Wavelet neural network classification of EEG signals by using AR model with MLE preprocessing,” *Neural Networks*, vol. 18, no. 7, pp. 985–997, 2005.
- [22] A. Subasi, “EEG signal classification using wavelet feature extraction and a mixture of expert model,” *Expert Systems with Applications*, vol. 32, no. 4, pp. 1084–1093, 2007.
- [23] N. Sadati, H. R. Mohseni, and A. Maghsoudi, “Epileptic seizure detection using neural fuzzy networks,” in *Proceedings of IEEE International Conference on Fuzzy Systems (FUZZY '06)*, pp. 596–600, Vancouver, BC, Canada, July 2006.
- [24] A. A. Dingle, R. D. Jones, G. J. Carroll, and W. R. Fright, “A multistage system to detect epileptiform activity in the EEG,” *IEEE Transactions on Biomedical Engineering*, vol. 40, no. 12, pp. 1260–1268, 1993.
- [25] A. T. Tzallas, P. S. Karvelis, C. D. Katsis, D. I. Fotiadis, S. Giannopoulos, and S. Konitsiotis, “A method for classification of transient events in EEG recordings: application to epilepsy diagnosis,” *Methods of Information in Medicine*, vol. 45, no. 6, pp. 610–621, 2006.
- [26] F. I. M. Argoud, F. M. de Azevedo, J. M. Neto, and E. Grillo, “SADE³: an effective system for automated detection of epileptiform events in long-term EEG based on context information,” *Medical and Biological Engineering and Computing*, vol. 44, no. 6, pp. 459–470, 2006.
- [27] B. L. K. Davey, W. R. Fright, G. J. Carroll, and R. D. Jones, “Expert system approach to detection of epileptiform activity in the EEG,” *Medical and Biological Engineering and Computing*, vol. 27, no. 4, pp. 365–370, 1989.
- [28] P. E. McSharry, T. He, L. A. Smith, and L. Tarassenko, “Linear and non-linear methods for automatic seizure detection in scalp electro-encephalogram recordings,” *Medical and Biological Engineering and Computing*, vol. 40, no. 4, pp. 447–461, 2002.
- [29] N. Paivinen, S. Lammi, A. Pitkanen, J. Nissinen, M. Penttonen, and T. Gronfors, “Epileptic seizure detection: a nonlinear viewpoint,” *Computer Methods and Programs in Biomedicine*, vol. 79, no. 2, pp. 151–159, 2005.
- [30] N. Kannathal, U. R. Acharya, C. M. Lim, and P. K. Sadasivan, “Characterization of EEG—a comparative study,” *Computer Methods and Programs in Biomedicine*, vol. 80, no. 1, pp. 17–23, 2005.
- [31] L. D. Iasemidis and J. C. Sackellares, “Chaos theory and epilepsy,” *Neuroscientist*, vol. 2, no. 2, pp. 118–126, 1996.
- [32] D. E. Lerner, “Monitoring changing dynamics with correlation integrals: case study of an epileptic seizure,” *Physica D*, vol. 97, no. 4, pp. 563–576, 1996.
- [33] K. Lehnertz and C. E. Elger, “Spatio-temporal dynamics of the primary epileptogenic area in temporal lobe epilepsy characterized by neuronal complexity loss,” *Electroencephalography and Clinical Neurophysiology*, vol. 95, no. 2, pp. 108–117, 1995.
- [34] N. F. Güler, E. D. Übeyli, and İ. Güler, “Recurrent neural networks employing Lyapunov exponents for EEG signals classification,” *Expert Systems with Applications*, vol. 29, no. 3, pp. 506–514, 2005.
- [35] N. Kannathal, M. L. Choo, U. R. Acharya, and P. K. Sadasivan, “Entropies for detection of epilepsy in EEG,” *Computer Methods and Programs in Biomedicine*, vol. 80, no. 3, pp. 187–194, 2005.
- [36] H. Qu and J. Gotman, “A patient-specific algorithm for the detection of seizure onset in long-term EEG monitoring: possible use as a warning device,” *IEEE Transactions on Biomedical Engineering*, vol. 44, no. 2, pp. 115–122, 1997.
- [37] A. B. Gardner, A. M. Krieger, G. Vachtsevanos, and B. Litt, “One-class novelty detection for seizure analysis from intracranial EEG,” *Journal of Machine Learning Research*, vol. 7, pp. 1025–1044, 2006.
- [38] H. H. Lange, J. P. Lieb, J. Engel Jr., and P. H. Crandall, “Temporo-spatial patterns of pre-ictal spike activity in human temporal lobe epilepsy,” *Electroencephalography and Clinical Neurophysiology*, vol. 56, no. 6, pp. 543–555, 1983.
- [39] S. J. Schiff, D. Colella, G. M. Jacyna, et al., “Brain chirps: spectrographic signatures of epileptic seizures,” *Clinical Neurophysiology*, vol. 111, no. 6, pp. 953–958, 2000.
- [40] K. Lehnertz, R. G. Andrzejak, J. Arnhold, et al., “Nonlinear EEG analysis in epilepsy: its possible use for interictal focus localization, seizure anticipation, and prevention,” *Journal of Clinical Neurophysiology*, vol. 18, no. 3, pp. 209–222, 2001.
- [41] M. Le Van Quyen, J. Martinerie, V. Navarro, et al., “Anticipation of epileptic seizures from standard EEG recordings,” *The Lancet*, vol. 357, no. 9251, pp. 183–188, 2001.
- [42] A. B. Geva and D. H. Kerem, “Forecasting generalized epileptic seizures from the EEG signal by wavelet analysis and dynamic unsupervised fuzzy clustering,” *IEEE Transactions on Biomedical Engineering*, vol. 45, no. 10, pp. 1205–1216, 1998.
- [43] B. Boashash, M. Mesbah, and P. Golditz, “Time frequency detection of EEG abnormalities,” in *Time-Frequency Signal Analysis and Processing: A Comprehensive Reference*, chapter 15, pp. 663–670, Elsevier, Oxford, UK, 2003.
- [44] H. Hassanpour, M. Mesbah, and B. Boashash, “Time-frequency based newborn EEG seizure detection using low and high frequency signatures,” *Physiological Measurement*, vol. 25, no. 4, pp. 935–944, 2004.
- [45] B. Boashash and M. Mesbah, “Time-frequency methodology for newborn electroencephalographic seizure detection,” in *Applications in Time-Frequency Signal Processing*, A. Papandreou-Suppappola, Ed., chapter 9, pp. 339–369, CRC Press, Boca Raton, Fla, USA, 2003.
- [46] R. G. Andrzejak, K. Lehnertz, F. Mormann, C. Rieke, P. David, and C. E. Elger, “Indications of nonlinear deterministic and finite-dimensional structures in time series of brain electrical activity: dependence on recording region and brain state,” *Physical Review E*, vol. 64, no. 6, Article ID 061907, 8 pages, 2001.
- [47] H. H. Jasper, “Ten-twenty electrode system of the International Federation,” *Electroencephalography and Clinical Neurophysiology*, vol. 10, pp. 371–375, 1958.

-
- [48] R. L. Allen and D. W. Mills, *Signal Analysis: Time, Frequency, Scale, and Structure*, Wiley-IEEE Press, New York, NY, USA, 2004.
 - [49] F. Auger, P. Flandrin, P. Gonçalves, and O. Lemoine, *Time-Frequency Toolbox*, Rice University, CNRS, France, 1996.
 - [50] C. M. Bishop, *Neural Networks for Pattern Recognition*, Oxford University Press, Oxford, UK, 1995.